

### Measurements of Ambipolar Diffusion in Helium\*

MANFRED A. BIONDI AND SANBORN C. BROWN

Research Laboratory of Electronics, Massachusetts Institute of Technology, Cambridge, Massachusetts

(Received February 10, 1949)

Microwave techniques are applied to the study of the diffusion of electrons and positive ions in helium. For the electron and ion densities realized experimentally, the diffusion takes place ambipolarly; that is, the flow of charged particles of both signs is equalized by the space charge field which they set up. At 1 mm Hg pressure and 0.039-eV average energy, the measured value of the ambipolar diffusion coefficient,  $D_a$ , is 540 cm<sup>2</sup>/sec. The measured variation of  $D_a$  with gas density, energy of the particles, and diffusion container size and shape agrees closely with theory.

**A**MBIPOLAR diffusion is the simultaneous diffusion of electrons and positive ions in the presence of their own space charge fields. Although the theory of ambipolar diffusion has been investigated extensively, experimental measurements in the past have been difficult to interpret because of the presence of undesired secondary processes. The recent advancement of microwave technique has led to an experiment capable of giving quantitative results which may be compared with theory.

#### THEORY

The motion of positive ions and electrons in a gas under the action of concentration gradients and an electric field may be expressed as:

$$\Gamma_- = n_- \bar{v}_- = -D_- \nabla n_- - \mu_- E n_- \tag{1}$$

$$\Gamma_+ = n_+ \bar{v}_+ = -D_+ \nabla n_+ + \mu_+ E n_+ \tag{2}$$

where  $\Gamma$  represents particle current density;  $n$  is particle density;  $\bar{v}$  is the average drift velocity;  $D$ , the diffusion coefficient;  $\mu$ , the mobility; and  $E$ , the electric field. The subscripts refer to the positive ions and the electrons. If the only field present is that due to the space charge of the particles and if the particle densities are sufficiently large, then

$(n_+ - n_-) \ll n_-$ , and the currents  $\Gamma_+$  and  $\Gamma_-$  will be equal. Equations (1) and (2) simplify to

$$\Gamma = -D_a \nabla n \tag{3}$$

where  $\Gamma$  and  $n$  refer to either positive ions or electrons. The ambipolar diffusion coefficient,  $D_a$ , is defined by:

$$D_a = (D_+ \mu_- + D_- \mu_+) / (\mu_+ + \mu_-) \tag{4}$$

The particle continuity equation may be written

$$P = (\partial n / \partial t) + \nabla \cdot \Gamma \tag{5}$$

where  $P = \nu n$  is the rate of production of positive ions or electrons, and  $\nu$  is the production rate per electron.

When Eq. (3) is substituted into Eq. (5), we obtain

$$D_a \nabla^2 n + \nu n = \partial n / \partial t \tag{6}$$

Assuming an exponential decrease of  $n$  with a mean decay time,  $\tau$ , one has

$$\nabla^2 n + ((\nu / D_a) + (1 / D_a \tau)) n = 0 \tag{7}$$

The boundary condition which is applied to Eq. (7) is that  $n$  goes to zero at the walls. This condition leads to a series of characteristic values and characteristic functions for Eq. (7).

$$\nabla^2 n_m + n_m / \Lambda_m^2 = 0 \tag{8}$$

where the  $\Lambda_m$ 's are lengths which describe the size of the container with regard to diffusion loss and are called the characteristic diffusion lengths. The boundary condition is satisfactory as long as the mean free paths of the particles are small compared to the dimensions of the container.

The solution of the diffusion Eq. (7) is in general a sum of the characteristic functions of Eq. (8). To measure the diffusion, however, it is necessary to have a single function, corresponding to the lowest characteristic value, as the solution of Eq. (7). In the experiment, two intervals are used, one during which the gas is broken down and a steady state is set up ( $\nu \neq 0, \tau = \infty$ ), followed by a second in which there is no applied field and therefore no production

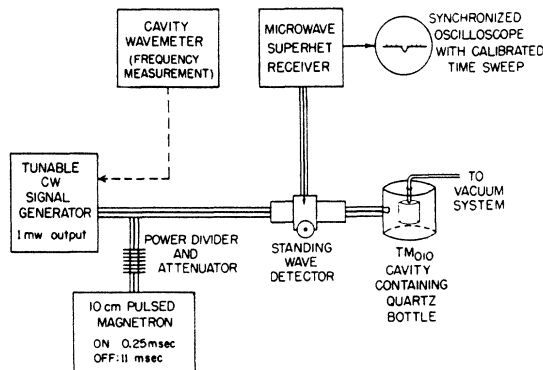


FIG. 1. Block diagram of the apparatus. The oscilloscope sweep is synchronized to start as the magnetron is turned off.

\* This work has been supported in part by the Signal Corps, the Air Materiel Command, and the ONR.

of ions or electrons ( $\nu=0$ ,  $\tau < \infty$ ), and the electron density decays. Measurements of  $n$  as a function of time are made during the second period. By making the ionization rate per electron,  $\nu$ , constant throughout the diffusion container, the lowest mode density distribution is generated during the first period, and maintained during the second period when  $\nu$  is zero. No data are taken until two milliseconds after the ionization ceases. This allows the electrons to come to thermal equilibrium with the gas and also insures that no higher modes are present during the measurements. Under these conditions, Eqs. (7) and (8) lead to

$$D_a = \Lambda_1^2 / \tau_1, \quad (9)$$

where  $\Lambda_1$  represents the lowest characteristic diffusion length. Thus the ambipolar diffusion coefficient may be determined by measuring the rate of decay of charge density in a container of known dimensions.

From kinetic theory,<sup>1</sup> the definition of the diffusion coefficient of a particle in terms of its mean free path,  $l$ , and velocity,  $v$ , is

$$D = (lv/3)_{av}, \quad (10)$$

where the average is over the distribution in velocity of the particles

Equations (4), (9), and (10) suggest the proper experimental variations to study. The effect of container size and shape, of gas density, and of the electron and ion energy upon measured values of  $D_a$  will be compared with theoretical predictions.

#### EXPERIMENTAL METHOD

The experimental method consists of measuring the mean decay time of charge density in a container of known dimensions by observing the change of the resonant wave-length of a microwave cavity enclosing the container. Provided that  $\sigma_i \ll \epsilon_0(2\pi c/\lambda_0)$  and  $\sigma_r \ll \sigma_i$ , the change in resonant wave-length of a cavity due to a complex conductivity within the cavity is given by<sup>2</sup>

$$\begin{aligned} \Delta\lambda/\lambda &= (\lambda_0 - \lambda)/\lambda \\ &= - \left( \lambda_0 \int_V \sigma_i E^2 dv \right) / \left( 4\pi c \epsilon_0 \int_V E^2 dv \right). \quad (11) \end{aligned}$$

$\lambda$  represents the resonant wave-length of the cavity with electrons inside;  $\lambda_0$  is the resonant wave-length of the cavity in the absence of electrons;  $\sigma_i$  and  $\sigma_r$  are the imaginary and real parts of the conductivity due to the electrons;  $E$  is the electric field in the cavity;  $c$  is the velocity of light, and  $\epsilon_0$  is the permittivity of free space. The relation between  $\sigma_i$

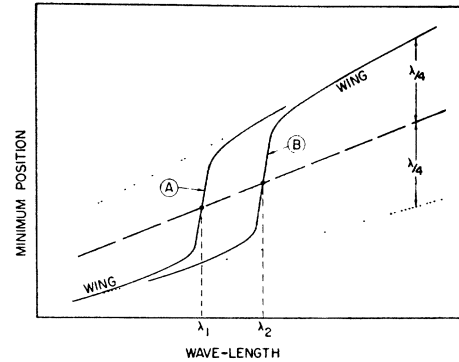


FIG. 2. Position in the coaxial line of a particular minimum of the standing wave pattern as a function of wave-length.

and electron density is given by

$$\sigma_i = -ne^2\lambda/2\pi mc, \quad (12)$$

where  $n$  is the electron density, and  $e$  and  $m$  are the charge and mass of the electron, respectively. For ambipolar diffusion, where the electron and the positive ion densities are nearly equal, the contribution to  $\sigma_i$ , and hence to  $\Delta\lambda$ , of the positive ions is negligible because of their large mass. Substituting Eq. (12) into Eq. (11) and integrating, one finds that

$$\Delta\lambda = C\lambda^2\bar{n}. \quad (13)$$

$C$  is a geometrical coefficient which takes into account the distribution of electron density and electric field in the cavity;  $\bar{n}$  is the average electron density within the quartz bottle. Thus the electron density within the cavity is related to the change of resonant wave-length of the cavity.

The experimental arrangement is shown in Fig. 1. Helium of a high degree of purity is introduced in the quartz bottle in the cavity. The vacuum system used in the experiment is thoroughly outgassed before each run. The quartz bottle in which the diffusion measurements are made is baked at 500°C, and a charcoal trap in the system is baked at 200°C for several days. For each run, a one liter flask of Air Reduction Sales Company spectroscopically pure<sup>3</sup> helium is used. When the system is isolated from the pumps by a mercury cut-off, a vacuum of between  $10^{-7}$  mm and  $10^{-6}$  mm is maintained for at least five hours (the maximum duration of a run). The helium in the quartz bottle is ionized by a 250-microsecond pulse from the 10-cm wave-length magnetron. A stationary charge distribution is reached during the pulse, and densities of the order of  $10^{10}$  to  $10^{11}$  electrons or ions/cc are produced. By placing the quartz bottle in the near-uniform field region of the

<sup>1</sup> J. Jeans, *The Dynamical Theory of Gases* (The Cambridge University Press, New York, 1921), p. 201.

<sup>2</sup> J. C. Slater, *Rev. Mod. Phys.* **18**, 481 (1946).

<sup>3</sup> Mass spectrographic analysis indicates none of the following impurities present within the resolution of the instrument (1 part in  $10^4$ ): H<sub>2</sub>, N<sub>2</sub>, O<sub>2</sub>, CO<sub>2</sub>, A, and Ne. However, the manufacturer believes that the contamination may be of the order of 1 part in  $10^6$ .

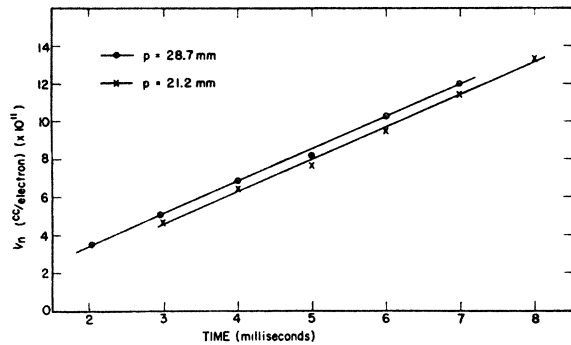


FIG. 3 Electron-positive ion recombination in helium at 0.039 eV average energy.

cavity, a density distribution is generated corresponding closely to the lowest mode of Eq. (8). The magnetron is then turned off for 11 milliseconds. The free electrons and ions lose energy by collision with gas atoms and come to equilibrium with the gas in less than 50 microseconds. Thus their energies during the measuring interval are thermal.

A small continuous signal is fed from the signal generator to the cavity. The field produced in the cavity by this signal does not appreciably alter the energy distribution of the electrons and ions. A standing wave pattern is set up in the coaxial line connecting the generator and the cavity. At the fixed frequency of the signal, the cavity impedance changes with time because of the decreasing electron density within the cavity. As a result, the minima of the standing wave pattern move along the coaxial line. At the time at which the resonant frequency of the cavity with residual electrons is equal to the signal frequency, the minima occur at so-called resonant minimum positions in the line. A probe inserted in the line at one of these points will receive a minimum signal at the time of resonance and a dip will occur on the oscilloscope trace. The method of determining the location of these resonant minimum positions will be discussed shortly.

By measuring the time at which resonance occurs (as indicated by the dip on the oscilloscope trace) for a number of different signal generator frequencies, the change of resonant wave-length of the cavity as a function of time is determined. Equation (13) then permits the determination of electron density as a function of time from which  $D_a$  may be found.

The positions of the minima of the standing wave pattern as a function of the resonant wave-length of the cavity and electrons are determined in the following manner: For the coupling between coaxial line and cavity used in this experiment, the position of a particular minimum of the standing wave pattern as a function of wave-length is given by the solid curves of Fig. 2. (For a discussion of this subject see reference 2.) Curve A represents the mini-

um position when the cavity contains an electron density,  $n_1$ , giving a resonant wave-length,  $\lambda_1$ . Curve B represents the minimum position when a smaller density,  $n_2$ , is present, giving a resonant wave-length,  $\lambda_2$ . The wings of the curve approach the dotted lines when  $\lambda$  is very different from the resonant wave-length. As indicated in the figure, the position of the minimum at resonance falls on the dashed curve which is called the resonant minimum curve.

One determines the resonant minimum curve by placing a shorting post at the center of the cavity, causing the resonant wave-length to be very greatly changed. As a result, the point at which the minimum curve crosses the dashed line is moved completely off the graph. The wings of the curve now coincide with the dotted lines over the wave-length range in which we are interested. The position of the minimum is measured as a function of wave-length using a slotted section and probe. By adding (or subtracting) a distance equal to  $\lambda/4$  to the ordinate of this curve, the resonant minimum curve for a particular minimum is determined.

#### CORRECTION FOR RECOMBINATION

The experimental measurement of the ambipolar diffusion coefficient is complicated by the presence of electron-positive ion recombination. Loss of particles to recombination may be expressed by

$$\partial n_+ / \partial t = \partial n_- / \partial t = -\alpha n_+ n_- = -\alpha n^2, \quad (14)$$

where  $\alpha$  is the recombination coefficient. Studies of this recombination in neon and argon (where ambipolar diffusion loss is secondary to recombination loss over the range of experimental variables used) indicate that  $\alpha$  is independent of pressure and energy at low energies.

At pressures above 20 mm in helium, the diffusion loss, which decreases with increasing pressure, be-

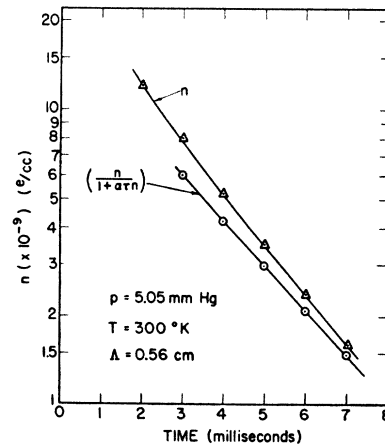


FIG. 4. Loss of electrons in helium by recombination and ambipolar diffusion.

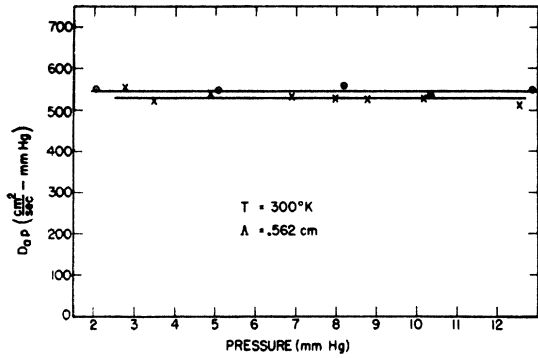


FIG. 5. Variation with pressure of the ambipolar diffusion coefficient for helium.

comes less important than the recombination loss, and Eq. (14) represents the principal loss of particles. The solution of Eq. (14) is

$$1/n = 1/n_0 + \alpha t, \quad (15)$$

where  $n_0$  represents the electron density at time  $t=0$ .

The recombination coefficient may be determined by measuring the slope of a reciprocal density *versus* time plot. The density is found by measuring  $\Delta\lambda/\lambda^2$  as a function of time and substituting in Eq. (13). Experimental data are shown in Fig. 3. The value of  $\alpha$  for helium is  $1.7 \times 10^{-8}$  (cc/ion-sec.).

At low pressures and low electron densities where diffusion loss outweighs recombination, the rate of decay of electron density is given approximately by:

$$\partial n / \partial t = -(n/\tau) - \alpha n^2, \quad (16)$$

where  $\tau$  is the mean decay time due to diffusion. The solution of this equation is

$$n/(1 + \alpha\tau n) = [n_0/(1 + \alpha\tau n_0)] \exp(-t/\tau), \quad (17)$$

where  $n_0$  represents the density at  $t=0$ . Equation (17) permits the correction of the data to find  $\tau$  and hence  $D_a$ . Figure 4 is a typical experimental curve. The upper curve shows the original data while the lower curve results when the recombination loss is subtracted. The time  $t=0$  was taken 3 milliseconds after the ionization ceased.

### EXPERIMENTAL RESULTS

Data of the type shown in Fig. 4 are taken as a function of pressure, temperature, and the size and shape of the container to complete the study of ambipolar diffusion. According to Eq. (10), at constant energy, the diffusion coefficient is proportional to the mean free path; that is,  $D_a p$  should be constant. Since the ions and electrons are in equilibrium with the gas, we control their energy by keeping the gas temperature constant. Figure 5 represents measurements on two different flasks of Air Reduction

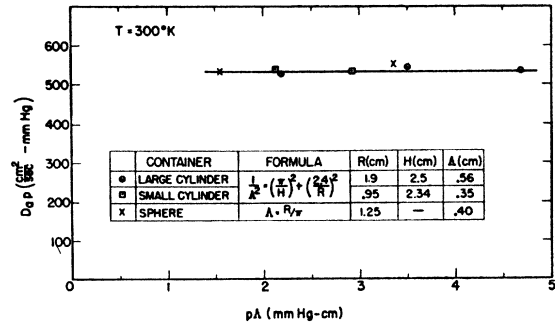


FIG. 6. Effect of the variation of the diffusion container size and shape upon the measured values of  $D_a$ .

Sales Company spectroscopically pure helium. Experimentally,  $D_a p$  is found to be independent of pressure within an error of less than 5 percent. The absolute magnitude of  $D_a p$  differs for the two samples by 3 percent.

The measured value of  $D_a$  should not depend on the size or the shape of the container in which the diffusion is taking place. Measurements of  $D_a$  were made in three containers whose dimensions are given in Fig. 6. Since different samples of helium give slightly different values of  $D_a$  (due to the presence of very small amounts of impurity), one cylinder was used as a reference, and measurements were made using one sample of helium for the large and the small cylinder and another sample for the large cylinder and the sphere. The results are plotted in Fig. 6. At constant energy, the value of  $D_a p$  is found to be independent of  $p\Lambda$  within 3 percent, and since  $D_a p$  has been shown to be independent of pressure, we conclude that the measured value of  $D_a$  does not depend on our choice of  $\Lambda$ .

Finally, the energy dependence of the ambipolar diffusion coefficient has been studied. Under the conditions of the experiment, the electrons and ions are in equilibrium with the gas and possess a Maxwellian energy distribution so that

$$D_{+}/\mu_{+} = D_{-}/\mu_{-} = kT/e, \quad (18)$$

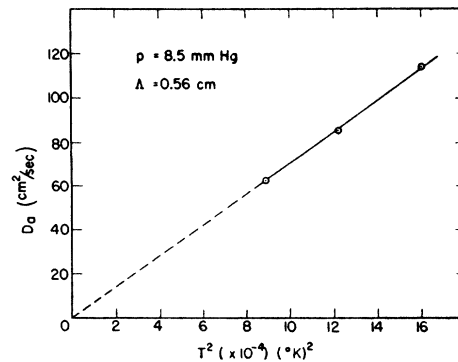


FIG. 7. Variation of the ambipolar diffusion coefficient with energy.

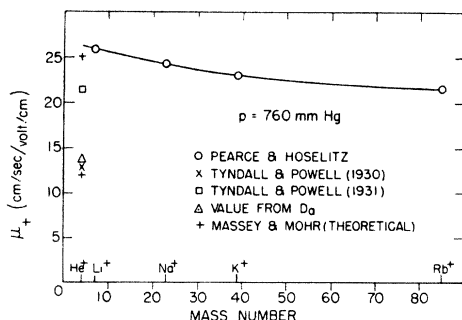


FIG. 8. Mobility of various positive ions in helium.

where  $T$  is the gas temperature. Under these conditions, Eq. (4) becomes

$$D_a = (2D_+\mu_-)/(\mu_- + \mu_+) \approx 2D_+, \quad (19)$$

because  $\mu_+$  is very much smaller than  $\mu_-$ . Positive ions in helium interact with the helium atoms according to an inverse fifth power law of force because of the induced dipole of the atom. Jeans<sup>4</sup> has shown that the diffusion coefficient for particles obeying this law of force is given by

$$D_+ \propto \bar{u}_+/n_g,$$

where  $\bar{u}_+$  is the average energy of the ion and  $n_g$  is the gas density. This means that the collision cross section for positive ions in helium varies as the reciprocal of the positive ion velocity. Experimental measurements of the collision cross section of positive ions in noble gases agree with the theoretical prediction.<sup>5</sup>

At constant pressure, the gas density varies inversely with the gas temperature so that under these conditions

$$D_a \propto T^2.$$

Experimental data are shown in Fig. 7. The energy range is small because of experimental limitations; however, the extrapolated curve passes through the origin in agreement with theoretical predictions.

#### DISCUSSION

The measured value of  $D_a p$  at 0.039-ev average energy is 540 (cm<sup>2</sup>/sec.)/(mm Hg). There is good agreement between experiment and theory with regard to the dependence of  $D_a$  on pressure, energy, and the size and shape of the diffusion container.

In the early part of the experimental work larger values of  $D_a$  were found, but the measured values of  $D_a$  became smaller as vacuum technique improved. We attribute this effect to the reduction of the amount of impurity with which the gas samples were contaminated by the vacuum system. If the

impurities exhibit electron attachment, they cause an additional loss of electrons which will lead to a spurious, high value of  $D_a$ . With present vacuum and gas preparation techniques, the impurity in the gas samples is not believed to be greater than 1 part in 10<sup>5</sup>. If this impurity has an attachment probability of 10<sup>-3</sup> attachments/collision, the effect on the measured value of  $D_a$  is only a few percent. Thus, the experiment has been done with what may be considered as a pure sample of helium.

The results of this experiment may help to resolve the discrepancy between the theoretical value of positive ion mobility in helium calculated by Massey and Mohr<sup>6</sup> and the experimentally determined value of Tyndall and Powell.<sup>7</sup> Equations (18) and (19) permit the conversion of the measured value of  $D_a$  to positive ion mobility. When our value of  $D_a$  is extrapolated to 760-mm pressure, a value of  $\mu_+ = 13.7$  (cm/sec.) per (volt/cm) is obtained. This value is represented by the triangular symbol in Fig. 8. Massey and Mohr calculate the mobility quantum mechanically, including the effect of charge transfer between the positive ion and atom on close approach, to be 12 (cm/sec.) per (volt/cm). Tyndall and Powell's measured value is 21.4 (cm/sec.) per (volt/cm). The quantum mechanical calculation of Massey and Mohr, omitting the effect of charge transfer, leads to a value of 25 (cm/sec.) per (volt/cm). Later work by Pearce<sup>8</sup> and Hoselitz<sup>9</sup> measured the mobility of various ions in helium. The results of their measurements are shown in Fig. 8. The theoretical value of Massey and Mohr, for the case in which charge transfer is neglected, lies quite close to the extrapolated mobility *versus* mass curve, as it should, since other ions cannot exhibit the charge transfer effect in helium. The theoretical value, including the charge transfer effect, lies close to both the value determined in the present experiment on  $D_a$ , and to the value of mobility which Tyndall and Powell measured in an earlier experiment published in 1930.<sup>10</sup>

The explanation of the difference between the values obtained in the two experiments of Tyndall and Powell is not clear. Their first experiment, in which the mobility was measured as 13 (cm/sec.) per (volt/cm) involved the generation of ions by  $\alpha$  particles. The second, in which the value 21.4 (cm/sec.) per (volt/cm) was obtained, generated ions by a point or wire-to-plane glow discharge. Brown<sup>11</sup> has shown that it is possible to generate appreciable amounts of He<sup>++</sup> in the inhomogeneous fields of this type of discharge.

<sup>6</sup> Massey and Mohr, Proc. Roy. Soc. **A144**, 188 (1934).

<sup>7</sup> Tyndall and Powell, Proc. Roy. Soc. **A134**, 125 (1931).

<sup>8</sup> Pearce, Proc. Roy. Soc. **A155**, 490 (1936).

<sup>9</sup> Hoselitz, Proc. Roy. Soc. **A177**, 200 (1941).

<sup>10</sup> Tyndall and Powell, Proc. Roy. Soc. **A129**, 162 (1930).

<sup>11</sup> S. C. Brown, Phys. Rev. **62**, 244 (1942).

<sup>4</sup> J. Jeans, *The Dynamical Theory of Gases* (The Cambridge University Press, New York, 1921), p. 247.

<sup>5</sup> C. Ramsauer and O. Beeck, Ann. d. Physik **87**, 1 (1928).

If the effect of charge transfer is neglected, the theoretical mobility of  $\text{He}^{++}$  should be nearly equal to that of  $\text{He}^+$ , since in doubling the charge, the mean free path between ion and atom is reduced to about half the value for the singly charged ion. On the other hand, the effect of total charge transfer

between  $\text{He}^{++}$  and  $\text{He}$  should be nearly absent. Therefore, it is suggested that Tyndall and Powell may actually have measured the mobility of  $\text{He}^{++}$  in their second experiment, inasmuch as their criterion was to select the fastest ion as the one which was to be measured.

PHYSICAL REVIEW

VOLUME 75, NUMBER 11

JUNE 1, 1949

## The Optical Constants of Germanium in the Infra-Red and Visible

W. H. BRATTAIN AND H. B. BRIGGS

*Bell Telephone Laboratories, Murray Hill, New Jersey*

(Received February 14, 1949)

Thin films of germanium have been evaporated on glass, quartz, and calcium fluoride slides. The thickness of these films ranged from  $4 \times 10^{-6}$  to  $1 \times 10^{-4}$  cm. Transmission of infra-red light through the films exhibited the usual interference phenomena, showing alternate maxima and minima as the wave-length was varied. From these maxima and minima the index of refraction of the films was determined. This index was 4.3 for  $\lambda$  greater than  $6 \times 10^{-4}$  cm wave-length. It increased to 5.2 at  $8.0 \times 10^{-5}$  cm and then fell off rapidly to 2.3 at  $4.0 \times 10^{-5}$  cm. To determine the values of the index and extinction coefficients in the visible region where the absorption is large, a wedge of germanium was made. Trans-

mission was then determined as a function of film thickness for several wave-lengths. The values of the optical constants in this region were then obtained by comparing these results with the theoretical transmission equations. The extinction coefficient increased from 0.4 at  $\lambda = 1 \times 10^{-4}$  cm to 2.8 at  $\lambda = 4 \times 10^{-5}$  cm. The density of the films was determined by an interferometric method and was found to be the same as bulk germanium. The real and imaginary parts of the dielectric constant for germanium are calculated and compared with the known results for silicon. The absorption bands for both elements are shown to be consistent with the electron band structure deduced from their semiconducting properties.

### I. EXPERIMENTAL RESULTS

A TYPICAL result for a germanium film on calcium fluoride is shown in Fig. 1. Here the transmission through the film is plotted as a function of the reciprocal of the wave-length  $\lambda$  in cm. The data were obtained with an infra-red spectrometer.<sup>1</sup> It is seen that seven orders of reinforcement were obtained before the absorption at shorter wave-lengths became too large. Another set of results on a thinner germanium film on glass is shown in Fig. 2. These results were obtained with a quartz spectrometer. Here both the transmission through the film at normal incidence, and the reflection from the film at  $45^\circ$  incidence are plotted against the wave-length  $\lambda$  in cm. Three orders of reinforcement are obtained and it is seen that the transmission maxima and minima correspond respectively to the reflection minima and maxima as they should. The well-known simple relations which govern the position of the maxima and minima are: The condition for transmission maxima

$$2nt = m\lambda, \quad (1)$$

where  $n$  is the index of refraction,  $t$  the thickness,  $m$  the order, and  $\lambda$  the wave-length; and the condition for transmission minimum

$$2nt = \frac{1}{2}(2m+1)/\lambda. \quad (2)$$

It is therefore obvious that if one knows the thickness of the film and the order number  $m$ , one can calculate the index  $n$  for every value of  $\lambda$  for which either a maxima or minima occurs. Since the order number<sup>2</sup> must be an integer, choice of the wrong order number makes a large difference in  $n$ . It is therefore easy to assign the correct order numbers if data are available on films of several thicknesses.

If the films are uniform in thickness and the density of the films is known, one can determine the thickness by weighing the films. The slides on which films of germanium were deposited were weighed before and after deposition of the film, and the area of the film was determined in each case. The uniformity in thickness of a film was determined by choosing a particular wave-length and measuring the transmission through different parts of the film. Since  $\lambda$  is fixed,  $n$  should be the same for all parts of the film, and therefore, if the thickness varies, the order  $m$  in Eq. (1) must vary. The percentage variation in the thickness of the film can be determined from the change in order:

$$\Delta t/t = \Delta m/m, \quad (3)$$

where  $t$  is the thickness and  $m$  the order for a particular spot on the film, and  $\Delta t$  is the change in thickness for a given change  $\Delta m$  in order as the position on the film is changed. By making such measurements on a single film for two different wave-lengths, the interpretation could be made

<sup>1</sup> We are indebted to P. P. Debye of these laboratories for use of the spectrometer to make these measurements.